Diabetes Publish Ahead of Print, published online February 27, 2008

Changes in gut microbiota control metabolic endotoxemia-induced inflammation in high-fat diet-induced obesity and diabetes in mice

Patrice D. Cani[1,2], Bibiloni Rodrigo[3], Claude Knauf[2], Aurélie Waget[2], Audrey M. Neyrinck[1], Nathalie M. Delzenne[1] and Rémy Burcelin[2]

[1] Unit of Pharmacokinetics, Metabolism, Nutrition and Toxicology, Université catholique de Louvain, Brussels, Belgium, [2] Rangueil Institute of Molecular Medicine, I^{2}MR, IFR31, Toulouse, France [3] Nestlé Research Center, Department of Nutrition and Health, Lausanne, Switzerland

Running Title: Gut flora, endotoxemia and inflammation

Corresponding Author:
Prof. Rémy Burcelin

Received for publication 3 October 2007 and accepted in revised form 25 February 2008.

Additional information for this article can be found in an online appendix at http://diabetes.diabetesjournals.org.

ABSTRACT

Diabetes and obesity are characterized by a low grade inflammation whose molecular origin is unknown. We previously determined first, that metabolic endotoxemia controls the inflammatory tone, body weight gain, and diabetes, second, that high-fat feeding modulates gut microbiota and the plasma concentration of lipopolysaccharide (LPS) i.e. metabolic endotoxemia. Hence, it remained to demonstrate whether changes in gut microbiota control the occurrence of metabolic diseases.

Objectives: first, to demonstrate that changes in gut microbiota, by the mean of antibiotic treatment, could be responsible for the control of metabolic endotoxemia, the low grade inflammation, obesity, and type 2 diabetes, and second to provide some mechanisms responsible for such effect.

Results: We found that changes of gut microbiota induced by an antibiotic treatment reduced metabolic endotoxemia and the ceacal content of LPS in both high-fat fed and *ob/ob* mice. This effect was correlated with reduced glucose intolerance, body weight gain and fat mass development, lower inflammation, oxidative stress, and macrophages infiltration marker mRNA expression in visceral adipose tissue. Importantly, high-fat feeding strongly increased intestinal permeability and reduced the expression of genes coding for proteins of the tight junctions. Furthermore, the absence of CD14 in *ob/ob CD14*$^{-/-}$ mutant mice mimicked the metabolic and inflammatory effects of antibiotics.

Conclusions: This new finding demonstrates that changes in gut microbiota controls metabolic endotoxemia, inflammation and associated disorders by a mechanism which could increase intestinal permeability. It would thus be useful to develop strategies for changing gut microbiota to control, intestinal permeability, metabolic endotoxemia and associated disorders.

KEY WORDS. Diabetes, obesity, gut microbiota, prebiotics, endotoxin, inflammation

ABBREVIATIONS. CT, control - CT-Ab, control antibiotic - HF, high-fat – HF-Ab, high-fat Antibiotic- LPS, lipopolysaccharide.

Environmental factors, such as a fat-enriched diet and a sedentary lifestyle, are the causes of the great prevalence of obesity and type 2 diabetes in the population (1). Diabetes and obesity are characterized by a low grade inflammation whose molecular origin is unknown (2;3). However, we have recently reported that moderate increase of plasma concentration of the inflammatory reagent, the bacterial lypopolysaccharide (LPS), increased during a fat-enriched diet, and defined metabolic endotoxemia (4). We demonstrated that LPS was responsible for the onset of metabolic diseases (4), since a continuous subcutaneous low rate infusion of LPS induced most, if not all, the features of metabolic diseases. Most importantly, the corresponding LPS receptor CD14 knockout mouse resisted the occurrence of the diseases. LPS is a major component of the outer membrane in Gram negative bacteria. Although the reasons of its increase in plasma during high-fat feeding were undetermined, its levels were closely correlated, but not causatively demonstrated, with changes in intestinal microbiota where the Gram negative to Gram positive ratio increased during high-fat feeding (4). Furthermore, dietary fibres, which reduce the impact of high-fat diet on the occurrence of the metabolic diseases (5), normalized the Gram-negative to Gram-positive ratio and plasma endotoxemia (6). This data strongly suggested that intestinal microbiota could be responsible for changes of metabolic endotoxemia and for the onset of the corresponding diseases. Although the causative link between intestinal bacteria, endotoxemia and metabolic disease was not shown. Gut microbiota has recently been proposed as an environmental factor involved in the control of body weight and energy homeostasis (7-12). Indeed, germ-free mice of the same age and genetic background as conventional mice fed with a normal chow diet had a 40% lower weight (11), whereas germ-free mice colonized with the gut microbiota derived from the conventional mice increased their fat mass and developed insulin resistance within 2 weeks. In addition, germ-free mice resisted high-fat diet-induced body weight gain, fat mass development, and had lower glycemia and insulinemia (9). Strikingly, these data did not provide any result with regard to the impact of the microflora on endotoxemia and inflammation. Altogether, this evidence suggests that changes in intestinal microbial composition could be responsible for increased endotoxemia in response to a high-fat diet which in turn would trigger the development of obesity and diabetes. Therefore, we aimed at changing the intestinal microbiota by means of an antibiotic treatment to reduce the elevated concentration of plasma LPS in high-fat diet fed mice and in *ob/ob* mice. We further studied some mechanisms through which intestinal microbiota changes metabolic endotoxemia and the corresponding metabolic consequences

RESEARCH DESIGN AND METHODS

Twelve-week-old male C57bl6/J mice (Charles River, Lyon, France) and six-week-old *ob/ob* (Ob, n=13) mice (C57bl6 background, Jackson Laboratory, Bar Harbor, ME, USA) were housed in a controled environment (inverted 12-h daylight-cycle, lights-off at 10:00A.M.) with free access to food and water. The mice were fed a control (CT,n=13) (A04, Villemoisson sur Orge, France) or a high-fat carbohydrate-free diet (HF,n=17) for 4 weeks. The role of the microflora was investigated by treating control (CT-Ab,n=13), high-fat fed (HF-Ab,n=17) or *ob/ob* (Ob-Ab,n=8) mice with antibiotics (1.0 g/l ampicillin (Sigma, St Louis, Mo) and 0.5 g/l neomycin (Sigma) in drinking water) during the experimental period. Ampicillin and neomycin are broad-

spectrum antibiotics that are poorly absorbed (or unabsorbed as in the case of neomycin) and thus without any systemic effects (13). The high-fat diet contained 72% fat (corn oil and lard), 28% protein, and <1% carbohydrate, as energy content (5). To generate the *ob/ob CD14*$^{-/-}$ mice, *CD14*$^{-/-}$ mice (C57bl6 background) were intercrossed with *ob*$^{+/-}$, and F1 double heterozygotes were then used to generate the *ob/ob CD14*$^{-/-}$ and *ob/ob* genotypes. All the following animal experimental procedures were validated by the local ethics committee: the Rangueil hospital animal ethics committee, and by the Université catholique de Louvain.

RNA extraction from caecal contents. Bacterial RNAs were extracted from caecal contents by using BioRobot-EZ1 (Qiagen, Germany), according to the manufacturer's instructions. In a nutshell, caecal contents were homogenized in a bead-beater for 2 min in a sterile microcentrifuge tube containing 0.3 g of glass beads and 750 µl of QIAzol lysis reagent. After the addition of 150 µl of chloroform:isoamylalcohol (24:1), the samples were vortexed for 15 sec and left to stand for 2-3 min at room temperature. Finally, the samples were centrifuged at 12,000 *g* for 15 min at 4°C and 300 µl of the supernatant was loaded into the BioRobot equipment.

Denaturing gradient gel electrophoresis (DGGE) profiles of caecal bacteria. Bacterial RNA was amplified by reverse transcription-PCR (RT-PCR) targeting the V3 region of the 16S rRNA gene, and using the universal bacterial primers HDA1-GC and HDA2, and a previously described programme (14) (HDA1-GC,5'-CGCCCGGGGCGCGCCCCGTGGCGG GGCGGGGGCGCGGGGGGACTCCTA CGGGAGGCAGCAGT-; and HDA2,5'-GTATTACCGCGGCTGCTGGCAC-3'). RT-PCR was performed by using a QIAGEN One-Step RT-PCR kit. Electrophoresis was performed with a DCode apparatus (Bio-Rad) and 6% polyacrylamide gels with a 30–55% gradient of 7M urea and 40% (v/v) formamide which increased in the direction of electrophoresis. Electrophoretic runs were in a TAE buffer (40 mM Tris, 20 mM acetic acid, 1 mM EDTA) at 130 V and 60° C for 270 min. Gels were stained with SYBR Safe 1× (Invitrogen, USA) for 30 min, rinsed with deionized water, and viewed by UV transillumination. DGGE profiles were compared by determining the Dice similarity coefficient (Dsc), and using the Bionumerics software package (version 4.01, Applied Maths) at a sensitivity of 1–2%.

Fecal analyses. The content of the cecum was vacuum dried. The remainder non digested carbohydrates, proteins, and lipids were quantified as described (15;16). The total LPS content was extracted and measured as described (17;18).

Quantitative RT-PCR quantification of Microbial caecal content. The caecal contents collected *post mortem* from mice were stored at -80°C. The QIAamp DNA Stool Minikit (Qiagen) was used to extract DNA from stool sample according to the manufacturer's instructions. The primers and probes used to detect *Bifidobacterium* spp. and *Lactobacillus* spp. were based on 16S rRNA gene sequences. The PCR amplification reactions were carried out as follows, 2 min at 50°C, 10 min at 95°C, followed by 45 cycles of 15 s at 95°C and 1 min at 60°C, and detection were carried out on an ABI Prism 7900 sequence detection system (Applied Biosystems). Each assay was performed in duplicate in the same run. The cycle threshold of each sample was then compared to a standard curve made by diluting genomic DNA (10-fold serial dilution) from cultures. Cell counts before DNA extraction were determined with the Neubauer hemocytometer. To determine the Sensitivity and specificity of the assays, the PCR assays were confirmed by using a set of intestinal bacterial species as controls. Group-specific primers based on

16 S rDNA sequences PCR assay are F-*Bifidobacterium*CGCGTCYGGTGTGAAAG, R-*Bifidobacterium*CCCCACATCCAGCATCCA, BHQ-1-bifidoAACAGGATTAGATACCC; F-*Lactobacillus*GAGGCAGCAGTAGGGAATCTTC, R-*Lactobacillus*GGCCAGTTACTACCTCTATCCTTCTTC, BHQ-1-lactoATGGAGCAACGCCGC. F-*Bacteroides-Prevotella*GAGAGGAAGGTCCCCCAC, R-Bacteroides-PrevotellaCGCTACTTGGCTGGTTCAG, VIC-CCATTGACCAATATTCCTCACTGCTGCCT-TAMRA.

Glucose tolerance tests. Oral (ogtt) glucose tolerance tests were performed as follows: six-hour fasted mice were injected with glucose by gavage (1g/kg of glucose, 20% glucose solution). Blood glucose was determined with a glucose meter (Roche Diagnostics, Meylan, France) on 3.5 µl of blood collected from the tip of the tail vein. In addition, to assess plasma insulin concentration, 20 µl of blood were sampled 30 min before and 15 min after the glucose challenge. The plasma was separated and frozen at -80°C.

Real-time quantitative PCR. *T*otal RNAs from each individual adipose tissues were prepared using the TriPure reagent (Roche, Basel, Switzerland) as described (5). cDNA was synthesised using reverse transcription kit (Promega corporation, Madison, WI, USA) from 1µg of total RNA. PCRs were performed with an AbiPrism 7000 Sequence Detection System instrument and software (Applied Biosystems, Foster City, CA, USA), as described (5). Primer sequences for the targeted mouse genes are the following F-TNF-αTGGGACAGTGACCTGGACTGT, R-TNF-αTTCGGAAAGCCCATTTGAGT; F-IL-1TCGCTCAGGGTCACAAGAAA, R-IL-1CATCAGAGGCAAGGAGGAAAAC; F-PAI-1ACAGCCTTTGTCATCTCAGCC, R-PAI-1CCGAACCACAAAGAGAAAGGA; F-RPL19GAAGGTCAAAGGGAATGTGTTCA, R-RPL19CCTTGTCTGCCTTCAGCTTGT; F-MCP-1GCAGTTAACGCCCCACTCA, R-MCP-1CCCAGCCTACTCATTGGGATCA, F-F4/80TGACAACCAGACGGCTTGTG, R-F4/80GCAGGCGAGGAAAAGATAGTGT; F-NADPHoxGGTTGGGGCTGAACATTTTTC, R-NADPHoxTCGACACACAGGAATCAGGAT; F-STAMP2GCATCTAGTGTTCCTGACTGGA, R-STAMP2TCAAATGCGGAATACCTTGCT, F-ZO-1ACCCGAAACTGATGCTGTGGATAG, R-ZO-1AAATGGCCGGGCAGAACTTGTGTA, F-OccludinATGTCCGGCCGATGCTCTC, R-OccludinTTTGGCTGCTCTTGGGTCTGTAT. The PCR conditions were: 2min at 50°C, 10min at 95°C followed by forty cycles of two-step PCR reaction denaturation at 95°C for 15s and annealing extension at 60°C for 60s. Each sample contained 0.5 to 5ng cDNA in 1X SYBR®Green PCR Master Mix (Applied Biosystems) and 200 or 300nM of each primer (Eurogentec, Verviers, Belgium) in a final volume of 25µl. The relative amount of each studied mRNA was normalized to RPL19 rRNA levels as housekeeping gene and the data was analyzed according to the $2^{-\Delta\Delta}$CT method.

Adipose tissue morphometry and staining. The mean relative proportion and mean surface area of the adipocytes was estimated by a point-counting technique, on paraffin-embedded as described (4).

Intestinal permeability in vivo. This measure is based on the intestinal permeability to 4000Da-fluorescent-

dextran (FD4000 Sigma-Aldrich, St. Louis, Mo, USA) as described (19). Briefly, 6 hours fasted mice were injected with FITC-dextran by gavage (600mg/kg body-weight, 125mg/ml). After 1h, 120µl of blood was collected from the tip of the tail vein. The blood was centrifuged at 4°C, 12000*g* for 3 minutes. Plasma was diluted in an equal volume of PBS (pH 7,4) and analyzed for FITC-dextran concentration with a fluorescence spectrophotometer (Perkin Elmer, HTS-7000 Plus-plate-reader, Wellesley, MA, USA) at the excitation wavelength of 485 nm and the emission wavelength of 535 nm. Standard curves for calculating the FITC-dextran concentration in the samples were obtained by diluting FITC-dextran in non treated plasma diluted with PBS (1:2vol/vol).

Biochemical analyses. Plasma LPS concentration was determined by using a kit based upon a Limulus amaebocyte extract (LAL kit endpoint-QCL1000, Cambrex BioScience, Walkersville, MD, USA), where samples were diluted 1/40 to 1/100 and heated for 10 minutes at 70°C. Internal control of recovery calculation was included in the assessment. Plasma insulin concentration was determined in 5µl of plasma by using an ELISA kit (Mercodia, Upssala, Sweden) and following the manufacturer's instructions. Visceral adipose tissue oxidative stress level was evaluated by measuring lipid peroxidation and reactive compounds such as Malondialdehyde (MDA) and 4-hydroxynonenal (4-HNE), natural byproducts of lipid peroxidation. The aldehydic secondary products of lipid peroxidation are accepted markers of oxidative stress. Thiobarbituric Acid Reactive Substances (TBARS) is a well-established assay for screening and monitoring lipid peroxidation. The adducts formed in samples, due to the reaction between MDA with Thiobarbituric Acid, were measured spectrophotometrically. TBARS levels were determined from a MDA equivalence standard.

Statistical analysis. Results are presented as mean ± SEM. The statistical significance of differences was analyzed by one-way ANOVA followed by post hoc (Bonferroni's multiple comparison test) or pearson's correlation using GraphPad Prism version 4.00 for windows (GraphPad Software, San Diego, CA, USA; www.graphpad.com). Data with different superscript letters are significantly different $P<0.05$, according to the post hoc ANOVA statistical analysis.

RESULTS

Antibiotic treatment associated changes in gut microbiota and endotoxemia during high-fat feeding. We previously showed that high-fat feeding changed gut microbiota and increased plasma LPS levels, as defined by metabolic endotoxemia (4). This was confirmed as assessed by the denaturing gradient gel electrophoresis (DGGE) analysis (**Fig.1A**). Therefore, to establish a cause and effect relationship according to which changes in gut microbiota initiate metabolic endotoxemia, we used large spectrum antibiotics to modify the intestinal microbial community in mice and assessed the main features of high-fat diet-induced metabolic disorders. A four-week antibiotic treatment strongly changed gut microbiota mRNA and bacterial content profile in both CT and HF treated mice (**Fig.1A, Table 1**). DGGE profiles clearly showed that cecal bacterial composition and/or metabolic activity were strongly affected after a four-week antibiotic treatment regardless of the diet (**Fig.1A**). Similarity analysis of DGGE profiles of cecal bacterial communities showed that the profiles of chow-fed animals and those of chow-fed animals treated with antibiotics were only 44% similar. This difference was even more dramatic between the high-fat (HF) and high-fat antibiotic treated mice (HF-Ab), where the profiles were only 22% similar. After antibiotic treatment, each individual

animal showed identical bacterial profiles (Dice's coefficient 100%). Moreover, we showed that high-fat diet dramatically changed the gut microbiota content. This was characterized by a strong reduction of some gram positive and negative bacteria (*Lactobacillus* spp., *Bifidobacterium* spp., and *Bacteroides-Prevotella* spp.) (**Table 1**). The reduced cecal microbiota content of HF antibiotic-treated mice only was associated with reduced metabolic endotoxemia to be similar to that of the CT mice (**Fig.1B**). Similarly, the Cecal endotoxin content per gram of cecal content was significantly decreased following antibiotic treatment (Cecal endotoxin content: CT 2.00^{a}±0.04 Log µg/g; CT-Ab 1.30^{b}±0.26 Log µg/g; HF 0.93^{c}±0.07 Log µg/g; HF-Ab 0.02^{d}±0.2 Log µg/g). Moreover, we found that high-fat diet-induced metabolic endotoxemia depended on a mechanism involved in the control of gut permeability. We demonstrated that high-fat feeding dramatically increased intestinal permeability (**Fig.1C**) by a mechanism associated with a reduced expression of epithelial tight junction proteins such as Z0-1 and Occludin (**Fig.1D-G**). Although, only a tendency was observed for occludin. This effect was completely restored by the antibiotic treatment. These data suggest that gut bacteria are involved in the control intestinal permeability and furthermore in the occurrence of metabolic endotoxemia.

Antibiotic treatment reduced the occurrence of adipose tissue inflammation, oxidative stress and macrophages infiltration markers in high-fat diet fed mice. To causally link changes of gut microbiota to high-fat diet-induced markers of metabolic disorders, we quantified the mRNA concentrations of PAI-1, IL-1 and TNF-α in visceral (mesenteric) adipose tissue. All mRNA concentrations were increased in high-fat diet-fed mice when compared to CT fed mice. This increase was totally blunted in the high-fat diet-fed antibiotic-treated mice (**Fig.2A, D, G**). Inflammation and metabolic disorders are frequently associated with oxidative stress in adipose depots (20-22). We found that high-fat feeding increased STAMP2 (21) and NADPHox mRNA concentrations and lipid peroxidation which were totally normalized by the antibiotic treatment (**Fig.2B, E, H**). Similarly, the mRNA concentrations of chemokine monocyte chemotactic protein (MCP)-1 and a marker specific of mature macrophages F4/80 were increased in HF mice and totally normalized by the antibiotic treatment (**Fig.2C, F**). The microflora therefore appears to be a key link between high-fat feeding, plasma LPS and visceral adipose tissue inflammation. As reported for the visceral adipose depots, the mRNA concentrations of PAI-1, IL-1, TNF-α and F4/80 were increased in the subcutaneous adipose depots of high-fat diet-fed mice as well (**Fig.3A, D, G, F**), whereas this increase was totally blunted in the high-fat diet-fed antibiotic-treated mice. However, no significant change was observed for STAMP2, NADPHox and MCP-1 mRNA (**Fig.3B, C, E**).

Metabolic endotoxemia positively correlated with inflammation, oxidative stress and macrophage infiltration markers. To identify whether the changes of gut microbiota and metabolic endotoxemia controlled visceral adipose tissue inflammation, oxidative stress and macrophages infiltration, we performed multiple correlation analyses between these parameters. Metabolic endotoxemia positively and significantly correlated with PAI-1, IL-1 and TNF-α, STAMP2, NADPHox, MCP-1 and F4/80 mRNA (**Fig.4A, B, C and supplemental Fig.1**). With the same aim in view, we performed other correlations and found that all inflammatory markers, oxidative stress and macrophage infiltration markers positively and significantly correlated with one another (**Fig.4D-I**), Altogether, these multiple correlations support a strong relationship between gut microbiota,

endotoxemia, inflammation and oxidative stress during high-fat diet feeding.

Antibiotic treatment prevented high-fat diet-induced adipocyte hypertrophy. We previously reported that a high-fat diet increased the adipocyte cell size (4) and here confirmed these data (**Fig.5A, B, D**). Furthermore we also assumed that it could be due to a LPS-dependent mechanism (4). Therefore, we wondered whether reduced metabolic endotoxemia, induced by the antibiotic treatment, was associated with changes in adipocyte cell size. The mean adipocyte size was reduced in HF antibiotic-treated mice when compared with HF untreated mice (**Fig.5A, B, D**). These changes were accompanied with a lower cell density when compared with all the groups (**Fig.5C**).

Antibiotic treatment improved metabolic parameters of diabetes and obesity in high-fat diet fed mice. HF feeding induced glucose intolerance as the blood glucose concentrations were all higher than those of the CT mice during the glucose challenge (**Fig.6A**). HF mice treated with antibiotics exhibited improved glucose tolerance when compared with untreated mice (**Fig.6A**). However, the blood glucose profiles and the calculated area under curve were still significantly different from the CT fed mice. Furthermore, glucose-induced insulin secretion, insulin resistance index, body weight gain, total energy intake, visceral and subcutaneous adipose weight, were significantly higher in high-fat diet-fed mice when compared with all the other groups (**Fig.6B-H**). All the parameters were corrected by the antibiotic treatment, except for the energy intake following high-fat diet feeding which was worsened during antibiotic treatment (**Fig.6F**). This increased energy intake could be related to an impaired energy harvesting. Fecal energy content per g of cecum content was similar between groups. It was 3.16^{a}±0.5 kcal/g, 3.28^{a}±0.04 kcal/g, 3.11^{a}±0.05 kcal/g, and 3.23^{a}±0.08 kcal/g, in CT, CT-Ab, HF, HF-Ab, respectively. However the total cecal content was decreased following high-fat feeding CT 0.45^{a}±0.02 vs HF 0.19^{c}±0.01g, and significantly increased after antibiotic treatment CT-Ab 1.36^{b}±0.08 and HF-Ab 0.82^{d}±0.03g. Consequently, the total cecal energy content was increased 4 fold in HF-Ab 2.85^{d}±0.05kcal when compared to HF mice 0.68^{c}±0.08kcal. A similar trend was observed in CT 1.42^{a}±0.38kcal vs CT-Ab 4.63^{b}±0.31kcal. The total cecal lipid content was six fold increased in HF-Ab 34.38^{c}±5.52mg when compared to HF mice 5.54^{a}±0.44mg. This increase was more moderate in CT 8.81^{a}±0.11mg vs CT-Ab 18.36^{b}±1.84mg.

Antibiotic treatment of ob/ob mice reduced endotoxemia. To assess the contribution of gut microbiota to the development of metabolic endotoxemia and inflammation regardless of the high-fat feeding, we turned to *ob/ob* mice. These animals are characterized by higher inflammatory tone and plasma LPS concentration whereas they are consuming a normal chow (23). Almost no bacterial RNAs were detected in any of the cecal contents of ob/ob mice treated with antibiotics, thus suggesting that similar to HF mice the antibiotic treatment had a dramatic effect on the *ob/ob* intestinal microbial population. This could be due to the increased food intake and hence antibiotic intake as well. Bacterial quantification confirms the DGGE profile and shows significant decrease in *Lactobacillus* spp., *Bifidobacterium* spp. and *Bacteroides-Prevotella* spp. (**Table 1**). Furthermore, our data showed that the treatment of *ob/ob* mice reduced metabolic endotoxemia (**Fig.7A, B**). However, endotoxemia still remained higher than CT values.

Antibiotic treatment of ob/ob mice lowered the mRNA concentration of adipose tissue inflammatory markers and metabolic parameters of diabetes and obesity. The mRNA concentrations of PAI-1 and F4/80 were significantly reduced in the visceral adipose depots and

to a lower extent in the subcutaneous adipose depots of *ob/ob* antibiotic-treated mice (**Fig.7H, I, L, M)**. Similarly, visceral adipose depot lipid peroxides, marker of oxidative stress, were two fold lower in antibiotic-treated mice (**Fig.7N**). Moreover, glucose intolerance (**Fig.7C**), insulin resistance index (**Fig.7F**), glucose-induced insulin secretion (**Fig.7E**), visceral and subcutaneous adipose tissue weights **(Fig.7J, K)** were reduced by the antibiotic treatment. However, no significant change of body weight was detected (**Fig.7G**).

The lack of the LPS receptor CD14 partially reverted inflammatory markers and metabolic parameters in ob/ob mice. We and others previously demonstrated that the lack of LPS receptor protects against the high-fat diet-induced adipose tissue inflammation and metabolic disorders (4;24-28). To demonstrate that the LPS receptor might be involved in the inflammatory phenotype of *ob/ob* mice we generated *ob/ob CD14*$^{-/-}$ mice. We showed here that in *ob/ob CD14*$^{-/-}$ mice PAI-1 and F4/80 mRNA concentrations were reduced in the visceral adipose depots (**Fig.7H, L**). This was accompanied by a reduction of oxidative stress markers (**Fig.7N**). All these parameters remained unchanged in the subcutaneous adipose depot when compared with *ob/ob* mice showing that CD14 mediated inflammation targeted visceral fat. Furthermore, blood glucose profiles, insulin resistance index, glucose-induced insulin secretion, visceral and subcutaneous adipose tissue weights, and lipid peroxidation were reduced in *ob/ob CD14*$^{-/-}$ when compared with *ob/ob* mice (**Fig.7C-N**).

DISCUSSION

We reported here that gut bacteria are involved in high-fat diet and *ob/ob* induced metabolic endotoxemia, adipose tissue inflammation and metabolic disorders. This effect could be mediated by a mechanism which could increase gut permeability and enhance LPS absorption. Antibiotic treatment significantly lowers plasma LPS levels, gut permeability, and the occurrence of visceral adipose tissue inflammation, oxidative stress, macrophages infiltration and metabolic disorders. We therefore conclude that gut microbiota could control intestinal permeability which determines the threshold at which metabolic endotoxemia-induced metabolic disorders occur.

We and others have recently demonstrated that the mechanisms of high-fat diet-induced inflammation and metabolic disorders were clearly linked to LPS (4;24-28). We here confirm these data and further demonstrate that this mechanism was linked to endotoxemia. We identified here that metabolic endotoxemia was due to changes in intestinal microbiota, since the antibiotic treatment, which dramatically reduced the local intestinal microbiota, restored normal plasma LPS values in high-fat diet-fed mice. High plasma LPS levels could result from an increased production of endotoxin by a change in gut microbiota (4;29). Evidently, the intestinal epithelium acts as a continuous barrier to avoid LPS translocation, but some endogenous or exogenous factors may alter this function. Among the factors promoting a leaky gut and increasing plasma LPS levels, alcohol consumption (30-34), immobilization stress (34;35), and radiation (36) have been put forward. Most importantly, in most of these studies antibiotic treatments were also administered and resulted in reduced plasma and cecal LPS levels. In addition to these factors, we further showed that reduced endotoxemia was due to a change in the microflora profile. High-fat feeding decreased the number of bifidobacteria (4;29). This group of bacteria has been shown to reduce intestinal LPS levels in mice and to improve the mucosal barrier function (37-39). Furthermore, we have shown that prebiotics increased the number of bifidobacteria and reduced the impact of

high-fat diet induced metabolic disorders (29). Interestingly, bifidobacteria do not degrade intestinal mucous glycoproteins like other pathogenic bacteria do. This effect promotes a healthier microvillus environment by preventing permeability and bacterial translocation (40;41). In the present study we further provide evidence that the mechanisms involved in the development of metabolic endotoxemia and the corresponding metabolic disorders in response to high-fat feeding are associated with an increased intestinal permeability. The modulation of gut bacteria following high-fat diet strongly increased intestinal permeability, by reducing the expression of genes coding for tight junction proteins ZO-1 and occludin. Moreover, our data demonstrate that gut bacteria are clearly involved in the present mechanism since antibiotic treated mice exhibited normal intestinal integrity whereas the mice were still eating a high-fat diet. We hence, suggest that high-fat feeding changes gut microflora which then increased intestinal LPS permeability (Fig 1C). It is noteworthy that the antibiotic treatment reduced the intestinal content in LPS which could contribute as well to the reduced metabolic endotoxemia. We report here that changes in feeding habits or the antibiotic treatment profoundly affects the fecal content in energy. The lipid content was dramatically increased in mice treated with antibiotics suggesting that intestinal flora contributes to energy harvesting or absorption. This observation is also supported by data from literature (7-12). Together, these data emphasize the role of gut microbiota in the development of high-fat diet-induced metabolic disorders.

These results demonstrate that the gut bacteria determines the threshold at which metabolic endotoxemia occurs during high-fat diet feeding. However, the role of gut microbiota on the development of metabolic endotoxemia-induced inflammation and metabolic disorders is poorly defined. Therefore, we characterized several inflammatory markers and found that the increase in PAI-1, IL-1 and TNF-α mRNA concentrations, following high-fat feeding, was completely abolished by the antibiotic treatment. This mechanism does not depend on the amount of fat ingested since it was even increased by the antibiotic treatment. Oxidative stress is frequently associated with inflammation and metabolic dysfunction in adipose depots (20-22). We similarly found that the antibiotic treatment totally normalized lipid peroxidation in the visceral adipose depots, the increased inflammatory/oxidative stress factor STAMP2 (21) and NADPHox mRNA concentration in the visceral and subcutaneous adipose depots. Furthermore, we found that antibiotic-treated mice exhibited normal F4/80 and MCP-1 mRNA concentrations in the visceral adipose depot. Our result are in agreement with data from the literature, since we and others have previously shown that high-fat feeding is associated with adipose tissue macrophages infiltration (F4/80 positive cells) and chemokine monocyte chemotactic protein (MCP)-1 (4;42;43). Moreover, our multiple correlation analyses strongly suggest that inflammation, macrophages infiltration, and oxidative stress markers are induced by LPS dependent mechanisms and controlled by the antibiotic treatment. We here also further demonstrated that the modulation of gut microbiota improved high-fat diet-induced glucose intolerance, body weight gain and fat mass development. These results are in line with our and other previous data showing that in the absence of metabolic endotoxemia or LPS receptor, dietary lipids are not sufficient to induce metabolic disorders (4;25;28;29).

To assess the contribution of gut microbiota to the development of metabolic endotoxemia and inflammation regardless of the high-fat feeding, we focused on *ob/ob* mice. These animals are indeed characterized by different gut

microbiota (8;12), higher inflammatory tone, and endotoxemia when compared with wild type mice (23). Antibiotic treatment dramatically changed the *ob/ob* mice gut microbiota, reduced *Lactobacillus* spp., *Bifidobacterium* spp., *Bacteroides-Prevotella* spp. and lowered metabolic endotoxemia. Furthermore, these parameters were associated with a significantly lower inflammatory tone in *ob/ob* antibiotic-treated mice. To demonstrate that the LPS receptor is involved in the regulation of inflammation and metabolic disorders in response to changes of gut microbiota, we therefore generated *ob/ob* mice lacking the LPS receptor CD14 (*ob/ob CD14*$^{-/-}$). Inflammation and macrophages infiltration markers were reduced in the visceral adipose depots and to a lower extent in the subcutaneous adipose depots of *ob/ob CD14*$^{-/-}$ mice. The latter set of data demonstrates that metabolic endotoxemia measured in *ob/ob* mice is at least in part, involved in the inflammatory phenotype. In *ob/ob* mice, both the lowering of metabolic endotoxemia, by means of the antibiotic treatment, or of LPS action, in the *ob/ob CD14*$^{-/-}$ mice, are associated with a significantly increased glucose tolerance and reduced visceral and subcutaneous adipose depots weight. Interestingly, we also found that *ob/ob* mice treated for four weeks with an endotoxin inhibitor (44) administered via osmotic mini-pumps, improved glucose tolerance and lowered adipose tissue fat mass (supplemental Fig.2). This pattern is similar to that observed in antibiotic-treated mice. This confirms that the gut microflora and the consequent increased bacteria-derived-factor LPS exerts a key role in the development of adipose depots and inflammation in *ob/ob* mice. Altogether, these data demonstrate that changes in gut microbiota and metabolic endotoxemia play a role in the *ob/ob* phenotype.

In the quest for non gut-dependent sources of endotoxemia, periodontitis could also be linked to the development of metabolic disorders (45). Several studies reported that the treatment of periodontitis with antibiotics was associated with improved metabolic parameters (46). Nevertheless, the impact of such antibiotic treatment on gut microbiota has not been investigated but could play a part in the improved metabolic phenotype.

To sum up, we have demonstrated first that in high-fat diet-fed mice the modulation of gut microbiota, is associated with an increased intestinal permeability which precedes the development of metabolic endotoxemia, inflammation and associated disorders (Fig.8). Second, we found that in *ob/ob* mice gut microbiota determines the concentration of plasma LPS, and is a mechanism involved in metabolic disorders. Altogether, we demonstrate that gut microbiota sets the threshold for metabolic endotoxemia.

ACKNOWLEDGEMENTS

We would like to thank Dr C. Feyt, and Dr G. Muccioli for helpful criticisms, and F. De Backer, A. Stroobants, A. Colom and C. Chabo for excellent technical assistance. PDC is Postdoctoral Researcher from the FRS-FNRS (Fonds de la Recherche Scientifique) Belgium, NMD and PDC and NMD are recipient of FSR subsides (Fonds speciaux de recherché, UCL, Belgium). RB is the recipient of subsides from the Nutritia Foundation, the AFERO, "Association Française Etude et de Recherche sur les obésités", l'Agence National de la Recherche (Programme ANR-05-PNRA-004 Nutrisens, PNRA-005.13 MitHyCal, PNRA- 30032006-01-03 Metaprofile), the INSERM (Institut National de la Santé et de la Recherche Médicale), the Université Paul Sabatier, the CESNA (Club d'étude du système nerveux autonome).

REFERENCES

1. Kahn,SE, Hull,RL, Utzschneider,KM: Mechanisms linking obesity to insulin resistance and type 2 diabetes. *Nature* 444:840-846, 2006
2. Hotamisligil,GS: Inflammation and metabolic disorders. *Nature* 444:860-867, 2006
3. Wellen,KE, Hotamisligil,GS: Inflammation, stress, and diabetes. *J Clin Invest* 115:1111-1119, 2005
4. Cani,PD, Amar,J, Iglesias,MA, Poggi,M, Knauf,C, Bastelica,D, Neyrinck,AM, Fava,F, Tuohy,KM, Chabo,C, Waget,A, Delmee,E, Cousin,B, Sulpice,T, Chamontin,B, Ferrieres,J, Tanti,JF, Gibson,GR, Casteilla,L, Delzenne,NM, Alessi,MC, Burcelin,R: Metabolic endotoxemia initiates obesity and insulin resistance. *Diabetes* 56:1761-1772, 2007
5. Cani,PD, Knauf,C, Iglesias,MA, Drucker,DJ, Delzenne,NM, Burcelin,R: Improvement of glucose tolerance and hepatic insulin sensitivity by oligofructose requires a functional glucagon-like peptide 1 receptor. *Diabetes* 55:1484-1490, 2006
6. Cani,PD, Neyrinck,AM, Fava,F, Knauf,C, Burcelin,RG, Tuohy,KM, Gibson,GR, Delzenne,NM: Selective increases of bifidobacteria in gut microflora improve high-fat-diet-induced diabetes in mice through a mechanism associated with endotoxaemia. *Diabetologia* 2007
7. Ley,RE, Turnbaugh,PJ, Klein,S, Gordon,JI: Microbial ecology: human gut microbes associated with obesity. *Nature* 444:1022-1023, 2006
8. Turnbaugh,PJ, Ley,RE, Mahowald,MA, Magrini,V, Mardis,ER, Gordon,JI: An obesity-associated gut microbiome with increased capacity for energy harvest. *Nature* 444:1027-1031, 2006
9. Backhed,F, Manchester,JK, Semenkovich,CF, Gordon,JI: Mechanisms underlying the resistance to diet-induced obesity in germ-free mice. *Proc Natl Acad Sci U S A* 104:979-984, 2007
10. Backhed,F, Ley,RE, Sonnenburg,JL, Peterson,DA, Gordon,JI: Host-bacterial mutualism in the human intestine. *Science* 307:1915-1920, 2005
11. Backhed,F, Ding,H, Wang,T, Hooper,LV, Koh,GY, Nagy,A, Semenkovich,CF, Gordon,JI: The gut microbiota as an environmental factor that regulates fat storage. *Proc Natl Acad Sci U S A* 101:15718-15723, 2004
12. Ley,RE, Backhed,F, Turnbaugh,P, Lozupone,CA, Knight,RD, Gordon,JI: Obesity alters gut microbial ecology. *Proc Natl Acad Sci U S A* 102:11070-11075, 2005
13. Ferrier,L, Berard,F, Debrauwer,L, Chabo,C, Langella,P, Bueno,L, Fioramonti,J: Impairment of the intestinal barrier by ethanol involves enteric microflora and mast cell activation in rodents. *Am J Pathol* 168:1148-1154, 2006
14. Tannock,GW, Munro,K, Harmsen,HJ, Welling,GW, Smart,J, Gopal,PK: Analysis of the fecal microflora of human subjects consuming a probiotic product containing Lactobacillus rhamnosus DR20. *Appl Environ Microbiol* 66:2578-2588, 2000
15. Futatsugi,A, Nakamura,T, Yamada,MK, Ebisui,E, Nakamura,K, Uchida,K, Kitaguchi,T, Takahashi-Iwanaga,H, Noda,T, Aruga,J, Mikoshiba,K: IP3 receptor types 2 and 3 mediate exocrine secretion underlying energy metabolism. *Science* 309:2232-2234, 2005
16. Jeejeebhoy,KN, Ahmad,S, Kozak,G: Determination of fecal fats containing both medium and long chain triglycerides and fatty acids. *Clin Biochem* 3:157-163, 1970
17. Goossens,D, Jonkers,D, Russel,M, Stobberingh,E, van den,BA, Stockbrugger,R: The effect of Lactobacillus plantarum 299v on the bacterial composition and metabolic activity in faeces of healthy volunteers: a placebo-controlled study on the onset and duration of effects. *Aliment Pharmacol Ther* 18:495-505, 2003

18. Goris,H, de,BF, van der,WD: Oral administration of antibiotics and intestinal flora associated endotoxin in mice. *Scand J Infect Dis* 18:55-63, 1986
19. Wang,Q, Fang,CH, Hasselgren,PO: Intestinal permeability is reduced and IL-10 levels are increased in septic IL-6 knockout mice. *Am J Physiol Regul Integr Comp Physiol* 281:R1013-R1023, 2001
20. Furukawa,S, Fujita,T, Shimabukuro,M, Iwaki,M, Yamada,Y, Nakajima,Y, Nakayama,O, Makishima,M, Matsuda,M, Shimomura,I: Increased oxidative stress in obesity and its impact on metabolic syndrome. *J Clin Invest* 114:1752-1761, 2004
21. Wellen,KE, Fucho,R, Gregor,MF, Furuhashi,M, Morgan,C, Lindstad,T, Vaillancourt,E, Gorgun,CZ, Saatcioglu,F, Hotamisligil,GS: Coordinated regulation of nutrient and inflammatory responses by STAMP2 is essential for metabolic homeostasis. *Cell* 129:537-548, 2007
22. Houstis,N, Rosen,ED, Lander,ES: Reactive oxygen species have a causal role in multiple forms of insulin resistance. *Nature* 440:944-948, 2006
23. Brun,P, Castagliuolo,I, Leo,VD, Buda,A, Pinzani,M, Palu,G, Martines,D: Increased intestinal permeability in obese mice: new evidence in the pathogenesis of nonalcoholic steatohepatitis. *Am J Physiol Gastrointest Liver Physiol* 292:G518-G525, 2007
24. Poggi,M, Bastelica,D, Gual,P, Iglesias,MA, Gremeaux,T, Knauf,C, Peiretti,F, Verdier,M, Juhan-Vague,I, Tanti,JF, Burcelin,R, Alessi,MC: C3H/HeJ mice carrying a toll-like receptor 4 mutation are protected against the development of insulin resistance in white adipose tissue in response to a high-fat diet. *Diabetologia* 50:1267-1276, 2007
25. Shi,H, Kokoeva,MV, Inouye,K, Tzameli,I, Yin,H, Flier,JS: TLR4 links innate immunity and fatty acid-induced insulin resistance. *J Clin Invest* 116:3015-3025, 2006
26. Song,MJ, Kim,KH, Yoon,JM, Kim,JB: Activation of Toll-like receptor 4 is associated with insulin resistance in adipocytes. *Biochem Biophys Res Commun* 346:739-745, 2006
27. Suganami,T, Mieda,T, Itoh,M, Shimoda,Y, Kamei,Y, Ogawa,Y: Attenuation of obesity-induced adipose tissue inflammation in C3H/HeJ mice carrying a Toll-like receptor 4 mutation. *Biochem Biophys Res Commun* 354:45-49, 2007
28. Tsukumo,DM, Carvalho-Filho,MA, Carvalheira,JB, Prada,PO, Hirabara,SM, Schenka,AA, Araujo,EP, Vassallo,J, Curi,R, Velloso,LA, Saad,MJ: Loss-of-function mutation in Toll-like receptor 4 prevents diet-induced obesity and insulin resistance. *Diabetes* 56:1986-1998, 2007
29. Cani,PD, Neyrinck,AM, Fava,F, Knauf,K, Burcelin,RG, Tuohy,KM, Gibson,GR, Delzenne,NM: Selective increases of bifidobacteria in gut microflora improves high-fat diet-induced diabetes in mice through a mechanism associated with endotoxemia. *Diabetologia*DOI 10.1007/s00125-007-0791-0, 2007
30. Nishida,J, Ekataksin,W, McDonnell,D, Urbaschek,R, Urbaschek,B, McCuskey,RS: Ethanol exacerbates hepatic microvascular dysfunction, endotoxemia, and lethality in septic mice. *Shock* 1:413-418, 1994
31. Adachi,Y, Moore,LE, Bradford,BU, Gao,W, Thurman,RG: Antibiotics prevent liver injury in rats following long-term exposure to ethanol. *Gastroenterology* 108:218-224, 1995
32. Enomoto,N, Ikejima,K, Yamashina,S, Hirose,M, Shimizu,H, Kitamura,T, Takei,Y, Sato,AN, Thurman,RG: Kupffer cell sensitization by alcohol involves increased permeability to gut-derived endotoxin. *Alcohol Clin Exp Res* 25:51S-54S, 2001

33. Enomoto,N, Ikejima,K, Bradford,B, Rivera,C, Kono,H, Brenner,DA, Thurman,RG: Alcohol causes both tolerance and sensitization of rat Kupffer cells via mechanisms dependent on endotoxin. *Gastroenterology* 115:443-451, 1998
34. Rivera,CA, Bradford,BU, Seabra,V, Thurman,RG: Role of endotoxin in the hypermetabolic state after acute ethanol exposure. *Am J Physiol* 275:G1252-G1258, 1998
35. Rivera,CA, Tcharmtchi,MH, Mendoza,L, Smith,CW: Endotoxemia and hepatic injury in a rodent model of hindlimb unloading. *J Appl Physiol* 95:1656-1663, 2003
36. Paulos,CM, Wrzesinski,C, Kaiser,A, Hinrichs,CS, Chieppa,M, Cassard,L, Palmer,DC, Boni,A, Muranski,P, Yu,Z, Gattinoni,L, Antony,PA, Rosenberg,SA, Restifo,NP: Microbial translocation augments the function of adoptively transferred self/tumor-specific CD8 T cells via TLR4 signaling. *J Clin Invest* 117:2197-2204, 2007
37. Wang,Z, Xiao,G, Yao,Y, Guo,S, Lu,K, Sheng,Z: The role of bifidobacteria in gut barrier function after thermal injury in rats. *J Trauma* 61:650-657, 2006
38. Griffiths,EA, Duffy,LC, Schanbacher,FL, Qiao,H, Dryja,D, Leavens,A, Rossman,J, Rich,G, Dirienzo,D, Ogra,PL: In vivo effects of bifidobacteria and lactoferrin on gut endotoxin concentration and mucosal immunity in Balb/c mice. *Dig Dis Sci* 49:579-589, 2004
39. Wang,ZT, Yao,YM, Xiao,GX, Sheng,ZY: Risk factors of development of gut-derived bacterial translocation in thermally injured rats. *World J Gastroenterol* 10:1619-1624, 2004
40. Caplan,MS, Miller-Catchpole,R, Kaup,S, Russell,T, Lickerman,M, Amer,M, Xiao,Y, Thomson,R, Jr.: Bifidobacterial supplementation reduces the incidence of necrotizing enterocolitis in a neonatal rat model. *Gastroenterology* 117:577-583, 1999
41. Ruseler-van Embden,JG, van Lieshout,LM, Gosselink,MJ, Marteau,P: Inability of Lactobacillus casei strain GG, L. acidophilus, and Bifidobacterium bifidum to degrade intestinal mucus glycoproteins. *Scand J Gastroenterol* 30:675-680, 1995
42. Weisberg,SP, McCann,D, Desai,M, Rosenbaum,M, Leibel,RL, Ferrante,AW, Jr.: Obesity is associated with macrophage accumulation in adipose tissue. *J Clin Invest* 112:1796-1808, 2003
43. Kanda,H, Tateya,S, Tamori,Y, Kotani,K, Hiasa,K, Kitazawa,R, Kitazawa,S, Miyachi,H, Maeda,S, Egashira,K, Kasuga,M: MCP-1 contributes to macrophage infiltration into adipose tissue, insulin resistance, and hepatic steatosis in obesity. *J Clin Invest* 116:1494-1505, 2006
44. Rustici,A, Velucchi,M, Faggioni,R, Sironi,M, Ghezzi,P, Quataert,S, Green,B, Porro,M: Molecular mapping and detoxification of the lipid A binding site by synthetic peptides. *Science* 259:361-365, 1993
45. Saito,T, Hayashida,H, Furugen,R: Comment on: Cani et al. (2007) Metabolic endotoxemia initiates obesity and insulin resistance: Diabetes 56:1761-1772. *Diabetes* 56:e20, 2007
46. Janket,SJ, Wightman,A, Baird,AE, Van Dyke,TE, Jones,JA: Does periodontal treatment improve glycemic control in diabetic patients? A meta-analysis of intervention studies. *J Dent Res* 84:1154-1159, 2005

TABLE 1. Bacterial quantification

	Lactobacillus spp. (number of cells/g of cecal content)	*Bifidobacterium* spp. (number of cells/g of cecal content)	*Bacteroides-Prevotella* spp. (number of cells/g of cecal content)
CT	$6.6\ 10^{8} \pm 3.4\ 10^{8\ a}$	$4.8\ 10^{6} \pm 1.1\ 10^{6\ a}$	$4.7\ 10^{8} \pm 5.8\ 10^{8\ a}$
HF	$3.0\ 10^{7} \pm 5.7\ 10^{6\ b}$	$5.9\ 10^{5} \pm 2.2\ 10^{5\ a}$	$1.2\ 10^{9} \pm 6.4\ 10^{8\ b}$
CT-Ab	$2.1\ 10^{5} \pm 3.8\ 10^{4\ c}$	$1.0\ 10^{4} \pm 4.9\ 10^{3\ b}$	$5.1\ 10^{7} \pm 4.4\ 10^{7\ c}$
HF-Ab	$3.9\ 10^{5} \pm 5.3\ 10^{4\ c}$	$4.5\ 10^{4} \pm 2.3\ 10^{4\ b}$	$2.1\ 10^{8} \pm 1.9\ 10^{8\ a}$
Ob-CT	$3.8\ 10^{9} \pm 1.2\ 10^{9\ a}$	$8.5\ 10^{6} \pm 3.8\ 10^{6\ a}$	$1.5\ 10^{8} \pm 7.6\ 10^{7}$
Ob-Ab	$1.8\ 10^{6} \pm 5.710^{5\ b}$	$1.4\ 10^{6} \pm 4.1\ 10^{5\ b}$	non detectable

Data are mean±SE. Data with different superscript letters are significantly different $P<0.05$, according to the post hoc ANOVA, or student test statistical analysis.

FIGURES LEGENDS

Figure 1. Antibiotic treatment associated changes in gut microbiota, intestinal permeability and endotoxemia during high-fat feeding
A*:** DGGE profiles generated from the caecal microbiota in normal-diet (CT), normal-diet and antibiotic (CT-Ab), high-fat diet (HF) or high-fat diet and antibiotic-fed (HF-Ab) mice for 4 weeks. Each number and profile corresponds to a different animal. Bar = Dice's similarity coefficient. ***B*:** Plasma endotoxin (LPS) concentration (EU/ml). Data are mean±SE. Data with different superscript letters are significantly different $P<0.05$, according to the post hoc ANOVA statistical analysis. ***C: Intestinal permeability assay: Plasma DX-4000-FITC (μg/ml). n.d.= non detectable concentration. ***D, F***: Epithelial tight junction proteins markers (ZO-1 and occludin mRNA concentrations, ***E, G:*** Correlations between intestinal permeability markers: plasma DX-4000-FITC and epithelial tight junction ZO-1 and occludin mRNA concentrations, $P<0.05$, *inset* corresponds to Pearson's r correlation and corresponding P value. Data are mean±SE. Data with different superscript letters are significantly different $P<0.05$, according to the post hoc ANOVA statistical analysis.

Figure 2. Antibiotic treatment reduced the occurrence of visceral adipose tissue inflammation, oxidative stress and macrophages infiltration markers in high-fat diet-fed mice.
Inflammation: PAI-1, IL-1, and TNF-α mRNA concentrations (***A, D*** and ***G***); Oxidative stress: STAMP-2 and NADPHox mRNA concentrations (***B*** and ***E***); Macrophages infiltration markers: MCP-1 and F4/80 mRNA concentrations (***C*** and ***F)***, visceral adipose tissue oxidative stress levels (lipid peroxides concentrations) (***H*)** in normal-diet (CT), normal-diet and antibiotics (CT-Ab), high-fat diet (HF) or high-fat diet and antibiotic-fed (HF-Ab) mice for 4 weeks. Data are mean±SE. Data with different superscript letters are significantly different $P<0.05$, according to the post hoc ANOVA statistical analysis.

Figure 3. Antibiotic treatment reduced the occurrence of subcutaneous adipose tissue inflammation, and macrophages infiltration markers in high-fat diet fed mice.
Inflammation: PAI-1, IL-1, and TNF-α mRNA concentrations (***A, D*** and ***G***); Oxidative stress: STAMP-2 and NADPHox mRNA concentrations (***B*** and ***E***); Macrophages infiltration markers: MCP-1 and F4/80 mRNA concentrations (***C*** and ***F***) in normal-diet (CT), normal-diet and antibiotics (CT-Ab), high-fat diet (HF) or high-fat diet and antibiotic-fed (HF-Ab) mice for 4 weeks. Data are mean±SE. Data with different superscript letters are significantly different $P<0.05$, according to the post hoc ANOVA statistical analysis.

Figure 4. Metabolic endotoxemia positively correlated with inflammation, oxidative stress and macrophage infiltration markers.
Correlations between plasma endotoxin (LPS, EU/ml) and PAI-1 (***A***), STAMP2 (***B***), and F4/80 (***C***) mRNA concentrations; correlations between PAI-1 mRNA concentrations and IL-1 (***D***), STAMP2 (***E***), and F4/80 mRNA (***F***) concentrations; correlations between NADPHox mRNA concentrations and PAI-1 (***G***), STAMP2 (***H***), and F4/80 mRNA (***I***) concentrations in the visceral adipose depots of normal-diet (CT), normal-diet and antibiotics (CT-Ab), high-fat diet (HF) or high-fat diet and antibiotic-fed (HF-Ab) mice for 4 weeks. $P<0.05$, *inset* corresponds to Pearson's r correlation and corresponding P value.

Figure 5. Antibiotic treatment prevented high-fat diet-induced adipocyte hypertrophy.
A: Adipocyte size distribution (%). ***B*:** Adipocyte mean area (μm^2). ***C*:** Cell density (arbitrary unit). ***D*:** Representative adipose tissue staining in normal-diet (CT), normal-diet and

antibiotics (CT-Ab), high-fat diet (HF) or high-fat diet and antibiotic fed (HF-Ab) mice for 4 weeks. Data are mean±SE. Data with different superscript letters are significantly different $P<0.05$, according to the post hoc ANOVA statistical analysis.

Figure 6. Antibiotic treatment improved metabolic parameters of diabetes and obesity in high-fat diet fed mice.

A: Plasma glucose (mmol/l) following an oral glucose load (1g/kg) in normal-diet (CT), normal-diet and antibiotics (CT-Ab), high-fat diet (HF) or high-fat diet and antibiotic fed (HF-Ab) mice for 4 weeks, the inset represents the area under curve (AUC) of the same groups. ***B*:** Plasma insulin concentration (pmol/l) 30 minutes before (-30) and 15 minutes after (15) oral glucose administration of the same groups. ***C*:** Insulin resistance index. ***D***: Glucose induced-insulin secretion after oral glucose administration. ***E***: Body weight gain. ***F*:** total energy intake. ***G***: subcutaneous adipose tissue weight (% of body weight). ***H***: Visceral adipose tissue weight (% of body weight) **in** normal-diet (CT), normal-diet and antibiotics (CT-Ab), high-fat diet (HF) or high-fat diet and antibiotic fed (HF-Ab) mice for 4 weeks. Data are mean±SE. Data with different superscript letters are significantly different $P<0.05$, according to the post hoc ANOVA statistical analysis.

Figure 7. Antibiotic treatment of *ob/ob* mice reduced endotoxemia. *ob/ob* mice treated with antibiotic and *ob/ob CD14*$^{-/-}$ mice exhibited lower mRNA concentration of adipose tissue inflammatory markers and improved metabolic parameters.

A*:** DGGE profiles generated from the caecal microbiota in *ob/ob* mice (Ob) or *ob/ob* mice treated with antibiotic (Ob-Ab) for 4 weeks. Each number and profile corresponds to a different animal. ***B*:** Plasma endotoxin (LPS) concentration (EU/ml). ***C*:** Plasma glucose (mmol/l) following an oral glucose load (1g/kg) in *ob/ob* (Ob), *ob/ob* treated with antibiotics (Ob-Ab) for 4 weeks, or *ob/ob 14*$^{-/-}$ mice, the inset represents the area under curve (AUC) of the same groups. ***D*:** Plasma insulin concentration (pmol/l) 30 minutes before (-30) and 15 minutes after (15) oral glucose administration of the same groups. ***E: Glucose induced-insulin secretion after oral glucose administration. ***F*:** Insulin resistance index. ***G***: Body weight gain. ***J*:** subcutaneous adipose tissue weight (% of body weight). ***K***: Visceral adipose tissue weight (% of body weight). ***H*** and ***L***: Visceral adipose tissue PAI-1, and F4/80 mRNA concentrations. ***I*** and ***M***: Subcutaneous adipose tissue PAI-1, and F4/80 mRNA concentrations in *ob/ob* (Ob), *ob/ob* treated with antibiotics (Ob-Ab) for 4 weeks, or *ob/ob 14*$^{-/-}$ mice. ***N*:** visceral adipose tissue oxidative stress levels (lipid peroxides concentrations) in the same groups. Data are mean±SE. Data with different superscript letters are significantly different $P<0.05$, according to the post hoc ANOVA statistical analysis.

Figure 8. Hypothesis for bacteria induced metabolic disease:

Upon excessive high-fat feeding, intestinal microflora changes. This is associated with an increased intestinal permeability. Consequently, endotoxemia increased and triggers inflammation and metabolic disorders.

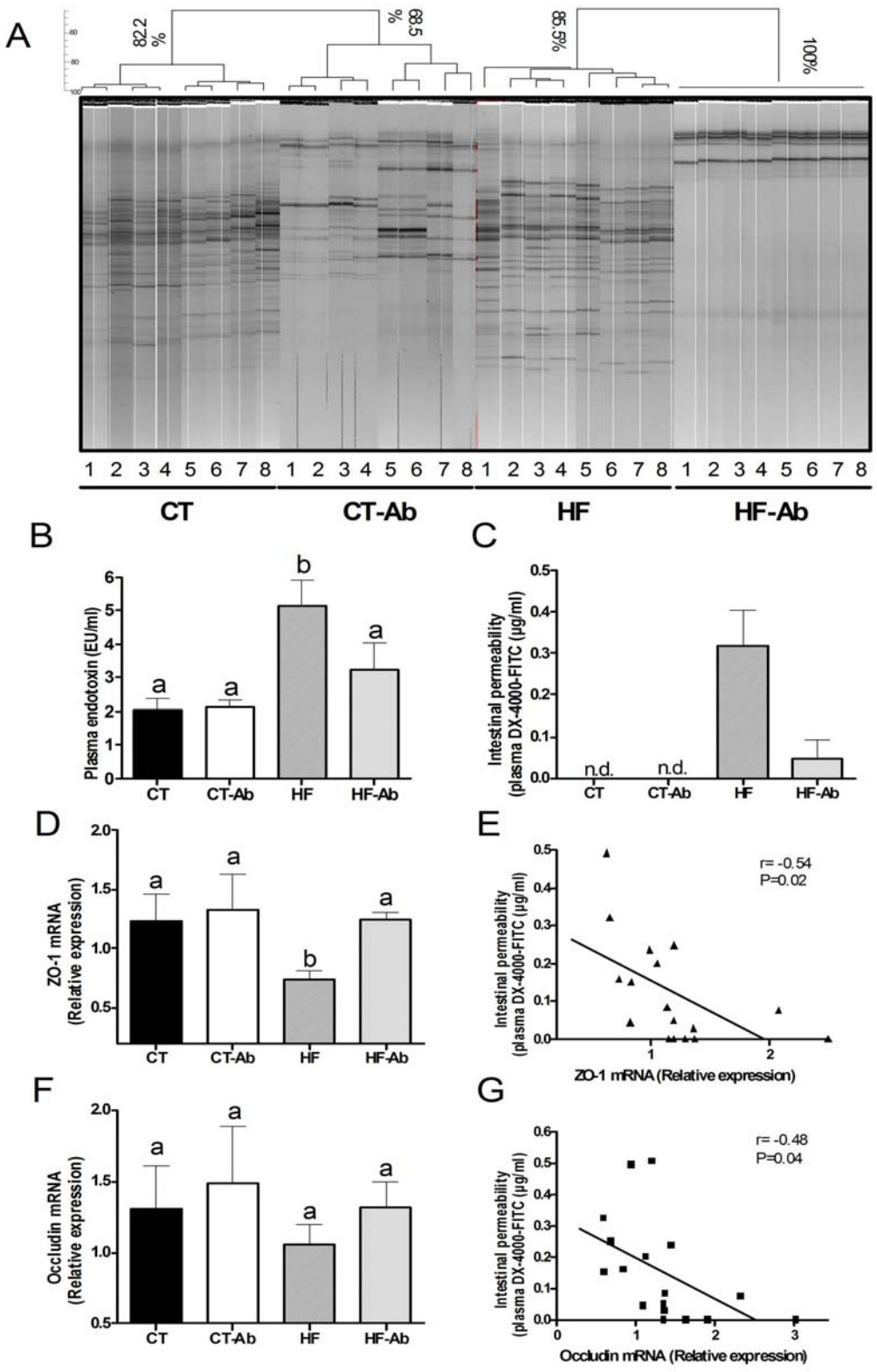
A
82.2 %
68.5 %
85.5%
100%
1 2 3 4 5 6 7 8 1 2 3 4 5 6 7 8 1 2 3 4 5 6 7 8 1 2 3 4 5 6 7 8
CT
CT-Ab
HF
HF-Ab
B
Plasma endotoxin (EU/ml)
a a b a
CT CT-Ab HF HF-Ab
C
Intestinal permeability (plasma DX-4000-FITC (µg/ml)
n.d. n.d.
CT CT-Ab HF HF-Ab
D
ZO-1 mRNA (Relative expression)
a a b a
CT CT-Ab HF HF-Ab
E
Intestinal permeability (plasma DX-4000-FITC (µg/ml)
r= -0.54
P=0.02
ZO-1 mRNA (Relative expression)
F
Occludin mRNA (Relative expression)
a a a a
CT CT-Ab HF HF-Ab
G
Intestinal permeability (plasma DX-4000-FITC (µg/ml)
r= -0.48
P=0.04
Occludin mRNA (Relative expression)

FIGURE 1

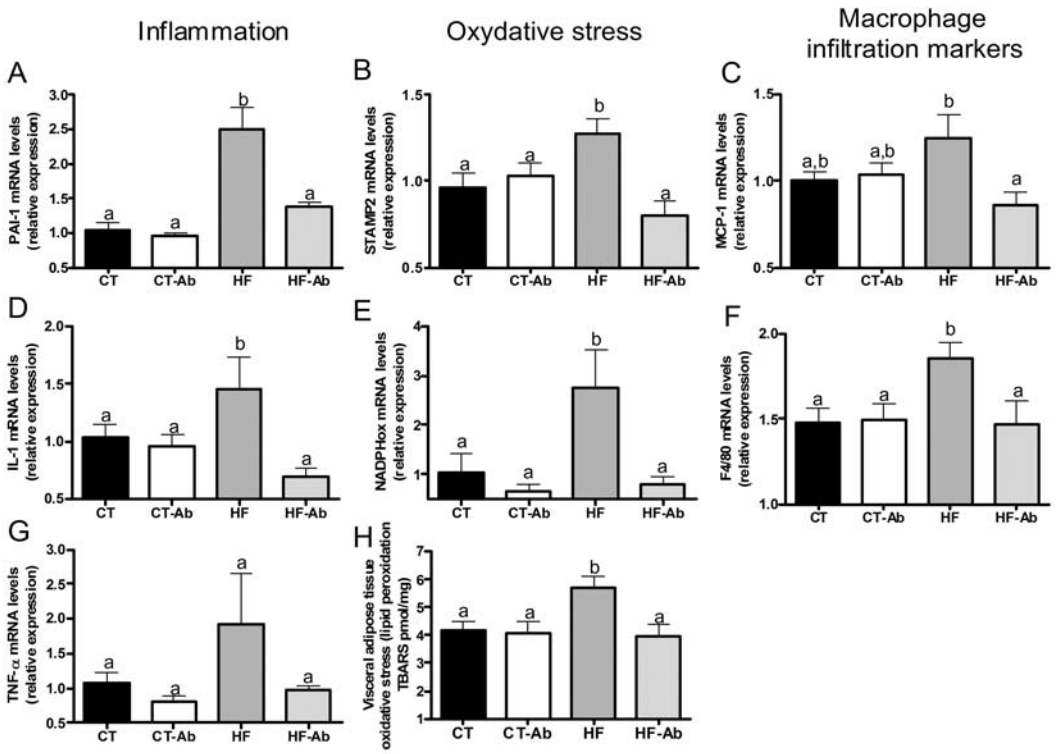
Inflammation
Oxydative stress
Macrophage infiltration markers
A
PAI-1 mRNA levels (relative expression)
B
STAMP2 mRNA levels (relative expression)
C
MCP-1 mRNA levels (relative expression)
D
IL-1 mRNA levels (relative expression)
E
NADPHox mRNA levels (relative expression)
F
F4/80 mRNA levels (relative expression)
G
TNF-α mRNA levels (relative expression)
H
Visceral adipose tissue oxidative stress (lipid peroxidation TBARS pmol/mg)
CT
CT-Ab
HF
HF-Ab

FIGURE 2

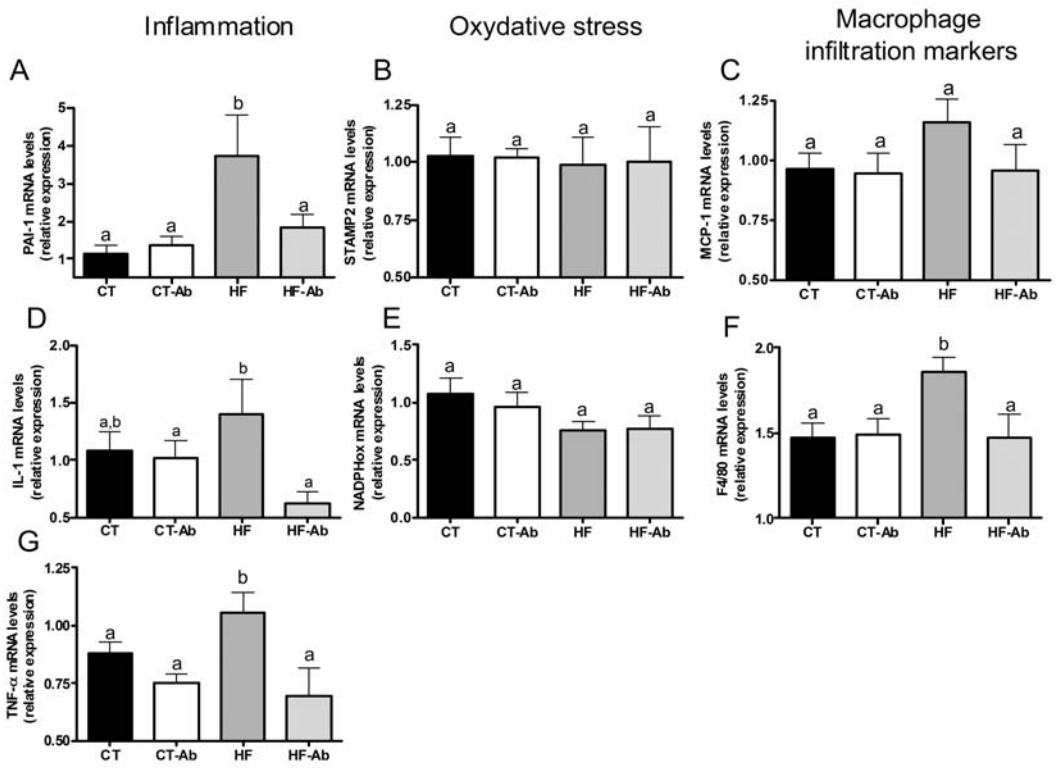
Inflammation
Oxydative stress
Macrophage infiltration markers
A
B
C
D
E
F
G
PAI-1 mRNA levels (relative expression)
STAMP2 mRNA levels (relative expression)
MCP-1 mRNA levels (relative expression)
IL-1 mRNA levels (relative expression)
NADPHox mRNA levels (relative expression)
F4/80 mRNA levels (relative expression)
TNF-α mRNA levels (relative expression)
CT
CT-Ab
HF
HF-Ab

FIGURE 3

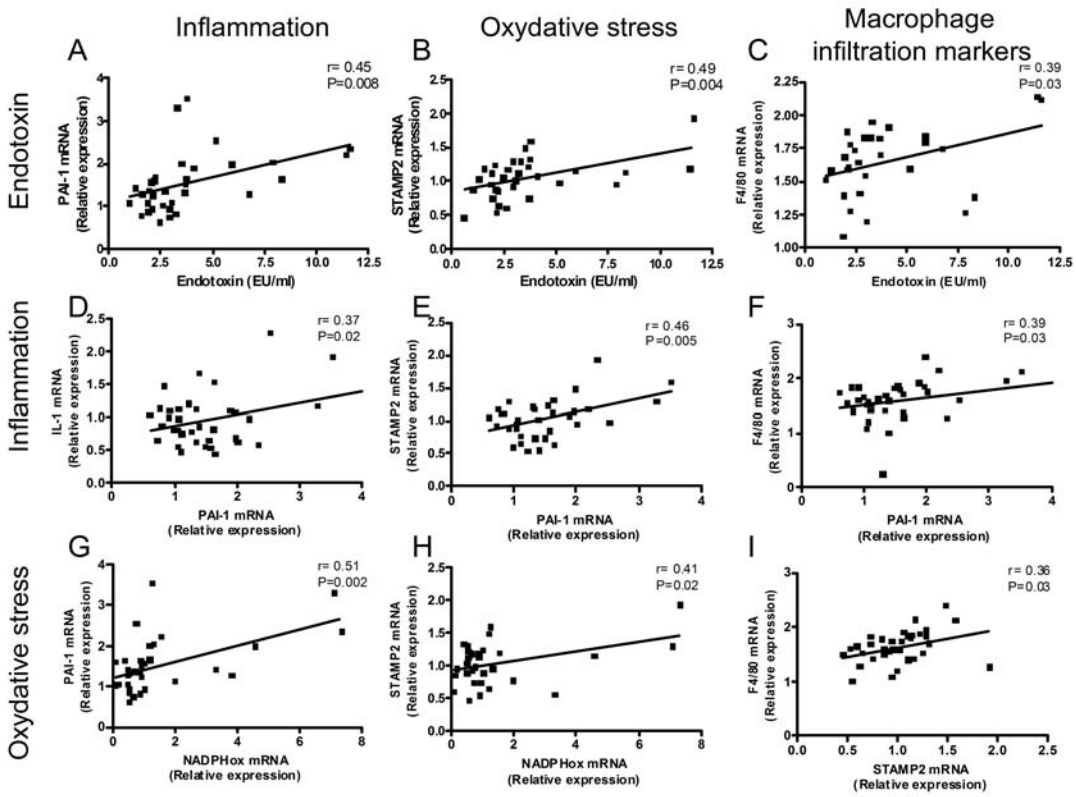
Inflammation
Oxydative stress
Macrophage infiltration markers
Endotoxin
Inflammation
Oxydative stress
A
B
C
D
E
F
G
H
I
r= 0.45
P=0.008
PAI-1 mRNA (Relative expression)
Endotoxin (EU/ml)
r= 0.49
P=0.004
STAMP2 mRNA (Relative expression)
Endotoxin (EU/ml)
r= 0.39
P=0.03
F4/80 mRNA (Relative expression)
Endotoxin (EU/ml)
r= 0.37
P=0.02
IL-1 mRNA (Relative expression)
PAI-1 mRNA (Relative expression)
r= 0.46
P=0.005
STAMP2 mRNA (Relative expression)
PAI-1 mRNA (Relative expression)
r= 0.39
P=0.03
F4/80 mRNA (Relative expression)
PAI-1 mRNA (Relative expression)
r= 0.51
P=0.002
PAI-1 mRNA (Relative expression)
NADPHox mRNA (Relative expression)
r= 0.41
P=0.02
STAMP2 mRNA (Relative expression)
NADPHox mRNA (Relative expression)
r= 0.36
P=0.03
F4/80 mRNA (Relative expression)
STAMP2 mRNA (Relative expression)

FIGURE 4

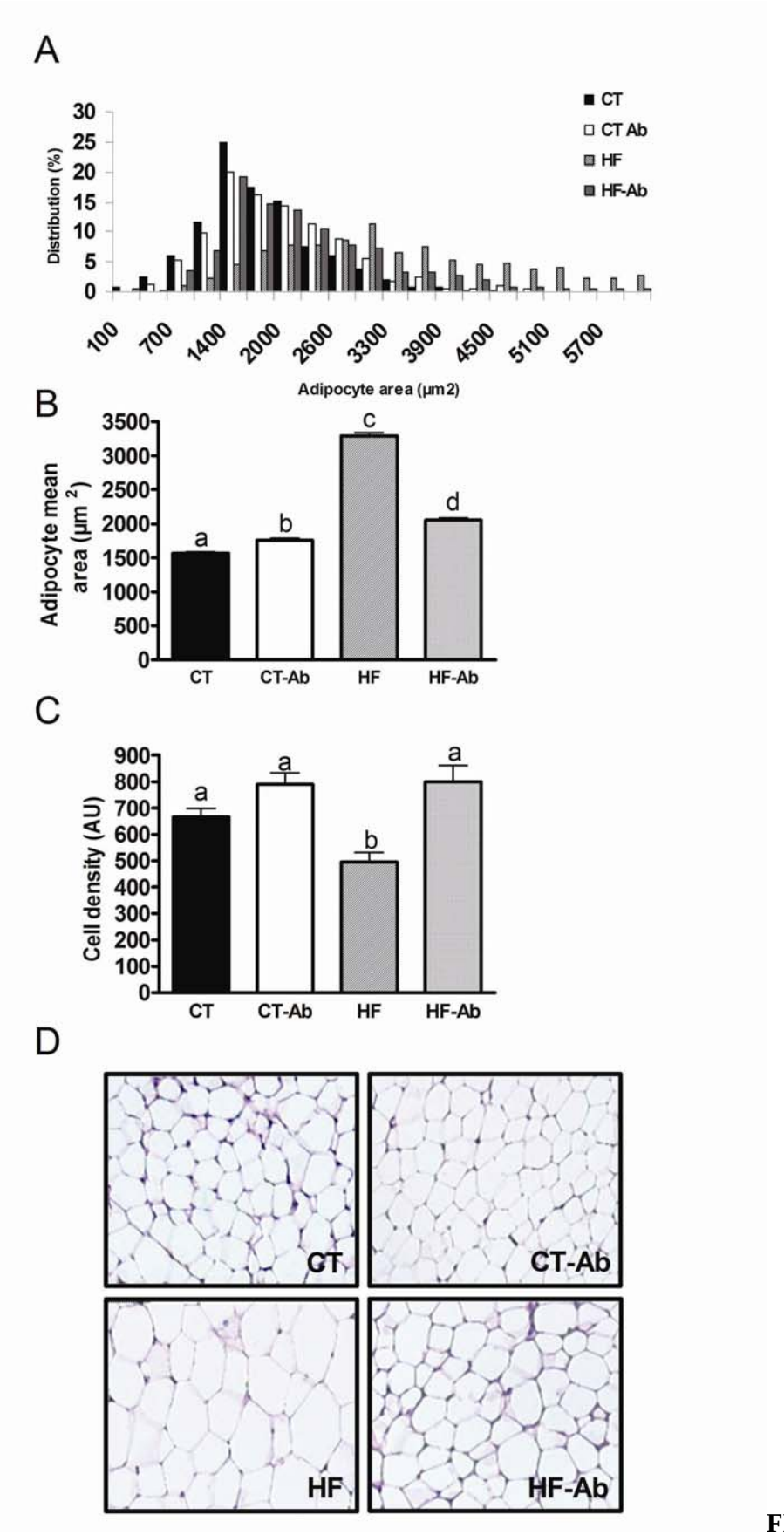
A
CT
CT Ab
HF
HF-Ab
Distribution (%)
30
25
20
15
10
5
0
100
700
1400
2000
2600
3300
3900
4500
5100
5700
Adipocyte area (µm2)
B
Adipocyte mean area (µm 2)
3500
3000
2500
2000
1500
1000
500
0
a
b
c
d
CT
CT-Ab
HF
HF-Ab
C
Cell density (AU)
900
800
700
600
500
400
300
200
100
0
a
a
b
a
CT
CT-Ab
HF
HF-Ab
D
CT
CT-Ab
HF
HF-Ab

FIGURE 5

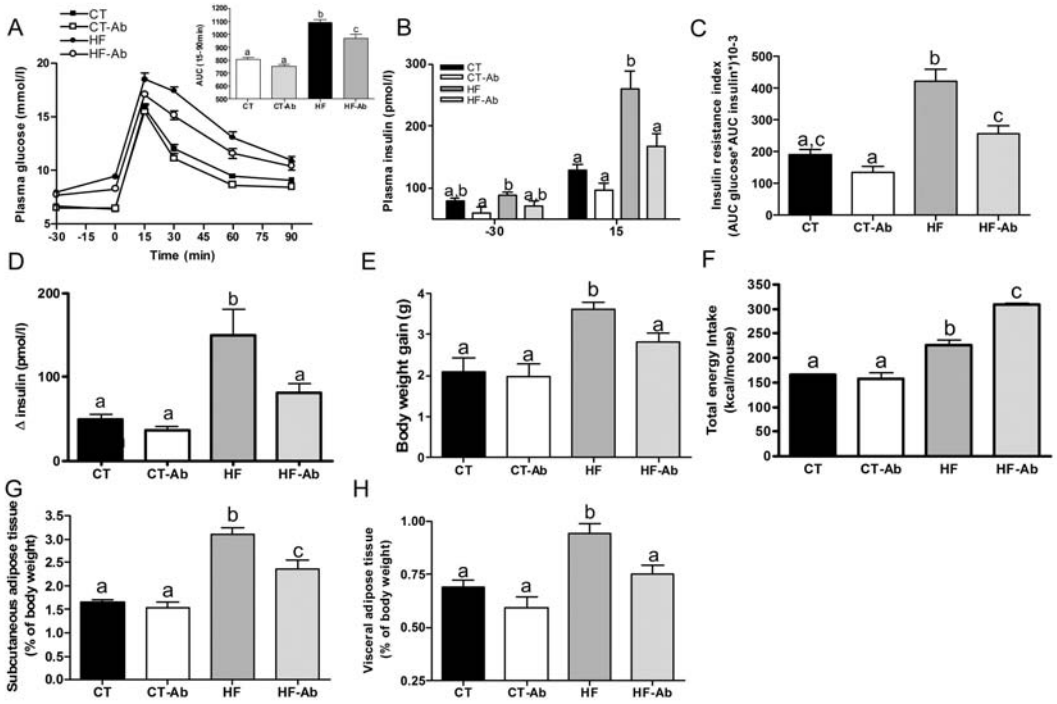
A
CT
CT-Ab
HF
HF-Ab
Plasma glucose (mmol/l)
Time (min)
B
Plasma insulin (pmol/l)
C
Insulin resistance index (AUC glucose*AUC insulin*)10-3
D
Δ insulin (pmol/l)
E
Body weight gain (g)
F
Total energy Intake (kcal/mouse)
G
Subcutaneous adipose tissue (% of body weight)
H
Visceral adipose tissue (% of body weight)

FIGURE 6

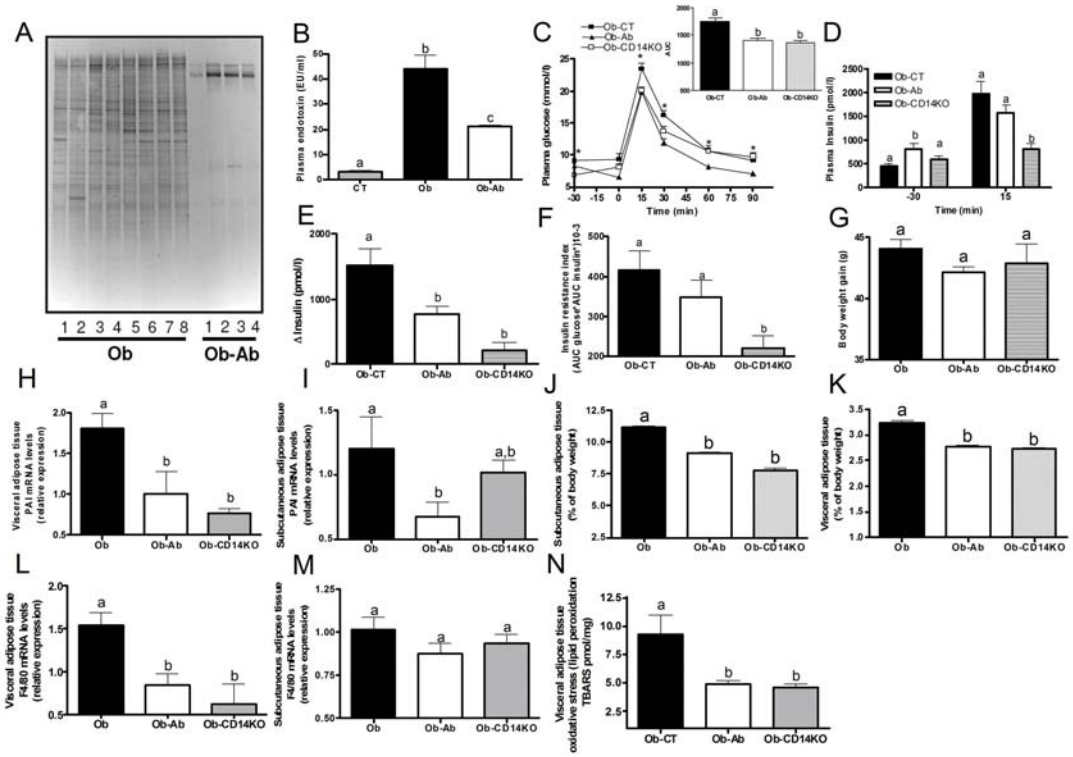
A
1 2 3 4 5 6 7 8
1 2 3 4
Ob
Ob-Ab
B
Plasma endotoxin (EU/ml)
CT
Ob
Ob-Ab
C
Ob-CT
Ob-Ab
Ob-CD14KO
Plasma glucose (mmol/l)
Time (min)
AUC
D
Ob-CT
Ob-Ab
Ob-CD14KO
Plasma Insulin (pmol/l)
Time (min)
E
ΔInsulin (pmol/l)
F
Insulin resistance index (AUC glucose*AUC insulin*10-3
G
Body weight gain (g)
H
Visceral adipose tissue PAI mRNA levels (relative expression)
I
Subcutaneous adipose tissue PAI mRNA levels (relative expression)
J
Subcutaneous adipose tissue (% of body weight)
K
Visceral adipose tissue (% of body weight)
L
Visceral adipose tissue F4/80 mRNA levels (relative expression)
M
Subcutaneous adipose tissue F4/80 mRNA levels (relative expression)
N
Visceral adipose tissue oxidative stress (lipid peroxidation TBARS pmol/mg)

FIGURE 7

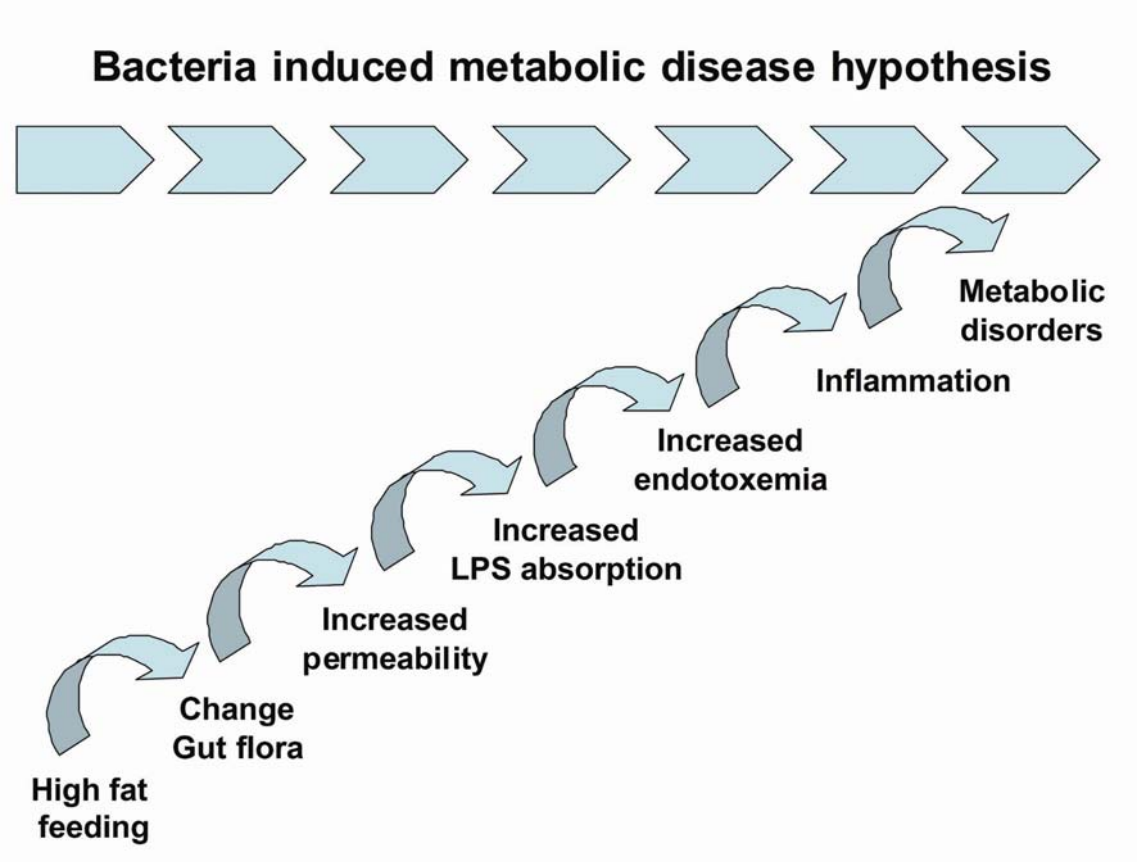
Bacteria induced metabolic disease hypothesis
High fat feeding
Change Gut flora
Increased permeability
Increased LPS absorption
Increased endotoxemia
Inflammation
Metabolic disorders

FIGURE 8